AOSS 555 Final Project: Modeling Seismic Wave Propagation with Radial Basis Functions

Trever Hines

April 27, 2015

Introduction

In recent years seismologists have become interested in using observable seismic waveforms to image the elastic properties of the Earth's interior. I use the term 'seismic waveform' to refer the the displacement history that can be observed on a seismogram over the course of hundreds of seconds following an earthquake. As with any inverse problem, imaging the elastic properties of the earth using seismic waveforms requires one to be able to solve the forward problem, that is, to compute the waveforms that would be predicted for a given realization of the Earth's interior. Researchers have used various numerical methods to solve this forward problem including finite difference methods, finite element methods, and spectral element methods (see Fichtner (2011) for a review of numerical methods in seismology). In this paper I will explore the potential for using radial basis functions (RBFs) to solve for the time dependent displacements throughout the earth following an earthquake.

One reason why RBFs are appealing is because they offer freedom in choosing the collocation points. In global seismology, one would ideally have a high clustering of collocation points at the core-mantle boundary, which is an interfaces where the elastic properties suddenly and drastically change. Additionally, the crust and the core have relatively low velocities and would require a higher density of nodes in accordance with the CFL criteria. RBFs seem to be appropriate for handling such heterogeneity in the Earth.

Another great advantage to RBFs is that they can be used to solve a problem on an arbitrarily complicated domain. Although the domain in global seismology is typically taken to be a sphere or a disk, more complicated geometries can arise in regional scale seismology problems where topography may need to be considered.

Problem Formulation

We can apply Newton's second law of motion to an infinitesimal parcel within a continuum to obtain displacements, $\boldsymbol{u}$, at any point $\boldsymbol{x}$ in the continuum as

$$\rho \frac{\partial^2 u_i}{\partial t^2} = \frac{\partial \tau_{ij}}{\partial x_j} + f_i, \tag{1}$$

where $\boldsymbol{\tau}$ and $\boldsymbol{f}$ are the stress tensor and body force per unit volume acting on point $\boldsymbol{x}$, respectively, and ρ is the density at point $\boldsymbol{x}$. Note that I have adopted Einstein notation where summations are implied by repeated indices. We can express eq. (1) in terms of $\boldsymbol{u}$ by using the definition of infinitesimal strain,

$$\varepsilon_{ij} = \frac{1}{2}\left(\frac{\partial u_j}{\partial x_i} + \frac{\partial u_i}{\partial x_j}\right), \tag{2}$$

and Hook's law in an isotropic medium,

$$\tau_{ij} = \lambda \delta_{ij} \varepsilon_{kk} + 2\mu \varepsilon_{ij}, \tag{3}$$

where λ and μ are Lamé parameters which we generally assume to be heterogeneous in the Earth. The differential equation being solved is then

$$\begin{aligned} \rho \frac{\partial^2 u_i}{\partial t^2} &= \frac{\partial}{\partial x_j}\left(\lambda \delta_{ij} \frac{\partial u_k}{\partial x_k} + \mu\left(\frac{\partial u_j}{\partial x_i} + \frac{\partial u_i}{\partial x_j}\right)\right) + f_i \\ &= \frac{\partial}{\partial x_i}\left(\lambda \frac{\partial u_k}{\partial x_k}\right) + \frac{\partial}{\partial x_j}\left(\mu\left(\frac{\partial u_j}{\partial x_i} + \frac{\partial u_i}{\partial x_j}\right)\right) + f_i \\ &= \frac{\partial \lambda}{\partial x_i}\frac{\partial u_k}{\partial x_k} + \lambda \frac{\partial^2 u_k}{\partial x_i x_k} + \frac{\partial \mu}{\partial x_j}\frac{\partial u_j}{\partial x_i} + \frac{\partial \mu}{\partial x_j}\frac{\partial u_i}{\partial x_j} + \mu \frac{\partial^2 u_j}{\partial x_j \partial x_i} + \mu \frac{\partial^2 u_i}{\partial x_j \partial x_j} + f_i. \end{aligned} \tag{4}$$

We impose free-surface boundary conditions, which means that

$$\boldsymbol{\tau} \cdot \hat{\boldsymbol{n}} = 0 \tag{5}$$

for all $\boldsymbol{x}$ on the surface of the Earth, which have surface normal vectors $\hat{\boldsymbol{n}}$. We can write the boundary conditions on $\boldsymbol{u}$ more explicitly as

$$\hat{n}_i \lambda \frac{\partial u_k}{\partial x_k} + \hat{n}_j \mu \left(\frac{\partial u_j}{\partial x_i} + \frac{\partial u_i}{\partial x_j}\right) = 0. \tag{6}$$

Although the equation that we are trying to solve looks daunting, if we consider a homogeneous medium, neglect body forces, and assume that displacement are in one direction and propagate in one direction, then we can see that eq. (4) reduces to the one dimensional wave equation. In particular, if displacements are in the direction of wave propagation then eq. (4) becomes

$$\frac{\partial^2 u}{\partial t^2} = \frac{\lambda + 2\mu}{\rho}\frac{\partial^2 u}{\partial x^2}, \tag{7}$$

where waves propagate at the P wave velocity, $\sqrt{(\lambda + 2\mu)/\rho}$. If displacements are perpendicular to the direction of wave propagation then eq. (4) reduces to

$$\frac{\partial^2 u}{\partial t^2} = \frac{\mu}{\rho}\frac{\partial^2 u}{\partial x^2}, \tag{8}$$

where waves propagate at the S wave velocity, $\sqrt{\mu/\rho}$.

When solving eq. (4), we assume the Earth is initially stationary and that all displacements are caused by an earthquake. Earthquakes are a sudden dislocation in the displacement field along a fault plane and so it seems reasonable that earthquakes should be imposed in this model by setting appropriate displacement boundary conditions on a prescribed fault plane. However, imposing a dislocation in the displacement field would undoubtedly cause numerical troubles. Fortunately, we can instead represent an earthquake as a collection of slightly offset point force couples, $\boldsymbol{F}^{(i,j)}$ (Aki & Richards, 2002). All nine unit force couples needed to represent a dislocation in three dimensional space are shown in figure 1. Approximating a dislocation as point force couples is reasonable if one is concerned with displacements far away from the source, i.e. seismic waves on a global scale. The finite length of a fault rupture must be considered if one is interested in near field displacements resulting from an earthquake. Even so, seismologists routinely represent earthquakes in terms of point force couples using what is known as a moment tensor, $\boldsymbol{M}$. The components of the moment tensor are

$$M_{ij} = |\boldsymbol{F}^{(i,j)}|d, \tag{9}$$

where d is the offset between the force couples, which would ideally be infinitesimally small. To give the moment tensor more tangible meaning, we can consider an isotropic compression source, such as a subsurface explosion, where the moment tensor representing that source would be

$$\boldsymbol{M} = M_o\boldsymbol{I}, \tag{10}$$

and M_o is the energy of the explosion. For our numerical simulation, we imposed an earthquake with moment tensor

$$\boldsymbol{M} = \begin{vmatrix} 0 & 10^{20} & 0 \\ 10^{20} & 0 & 0 \\ 0 & 0 & 0 \end{vmatrix} Nm, \tag{11}$$

which is equivalent to a Mw7.3 earthquake on a fault that is aligned with either the first or second coordinate axis.

We can represent the body force density for each force couple (without implied summations) as

$$\boldsymbol{f}^{(i,j)} = \frac{M_{ij}\hat{\boldsymbol{e}}_i}{d}\left(\delta\left(\boldsymbol{x} - \frac{d\hat{\boldsymbol{e}}_j}{2}\right) - \delta\left(\boldsymbol{x} + \frac{d\hat{\boldsymbol{e}}_j}{2}\right)\right), \tag{12}$$

where $\hat{\mathbf{e}}_i$ denotes a unit basis vector in direction i and δ is a three dimensional delta function, which can be taken to be a three dimensional Gaussian function with an infinitely small width. We can then represent the forcing term in 4 as

$$\boldsymbol{f} = \sum_{ij}\frac{M_{ij}\hat{\boldsymbol{e}}_i}{d}\left(\delta\left(\boldsymbol{x} - \frac{d\hat{\boldsymbol{e}}_j}{2}\right) - \delta\left(\boldsymbol{x} + \frac{d\hat{\boldsymbol{e}}_j}{2}\right)\right). \tag{13}$$

Although we circumvented to troubles of imposing a dislocation in the displacement field, we now face the difficulty of numerically representing a delta function. Indeed, the accuracy of our solution will come down to our ability to accurately represent a point force, which requires a very high density of collocation points. Using a desktop computer with 16 GB of RAM, we are only able to accurately represent a delta function as a 100 km wide Gaussian function, which is certainly not infinitesimally small compared to the Earth but it is the best we can do.

For the solutions presented in this paper, we assume that all energy is instantaneously released during an earthquake and $\boldsymbol{f}$ has no time dependence. This assumption may not be reasonable because large earthquakes could last for several minutes, which is on the timescale of seismic wave propagation.

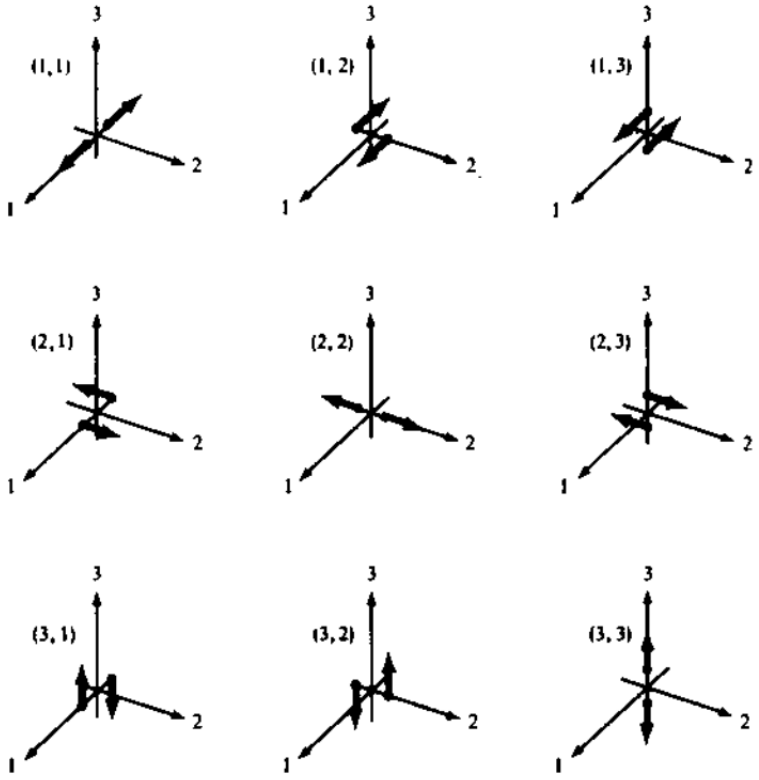

Figure 1: Unit force couples, $\hat{\boldsymbol{F}}^{(i,j)}$, that can be used to represent any type of dislocation on a fault (taken from Aki & Richards (2002))

Spectral Discretization

We will assume, for computational tractability but without loss of generality, that the domain is a two dimensional cross-section of the Earth and displacements are only in the plane of

that cross-section. After expanding the summation notation, eq. (4) can then be written as

$$\begin{vmatrix} \partial^2 u_1/\partial t^2 \\ \partial^2 u_2/\partial t^2 \end{vmatrix} = \begin{vmatrix} \partial_1\left((\lambda+2\mu)\partial_1 u_1\right) + \partial_2\left(\mu\partial_2 u_1\right) + \partial_1\left(\lambda\partial_2 u_2\right) + \partial_2\left(\mu\partial_1 u_2\right) \\ \partial_1\left(\mu\partial_2 u_1\right) + \partial_2\left(\lambda\partial_1 u_1\right) + \partial_2\left((\lambda+2\mu)\partial_2 u_2\right) + \partial_1\left(\mu\partial_1 u_2\right) \end{vmatrix} + \begin{vmatrix} f_1 \\ f_2 \end{vmatrix}, \tag{14}$$

where we use ∂_i to denote a derivative with respect to x_i. Likewise, the boundary conditions can be written as

$$\begin{vmatrix} 0 \\ 0 \end{vmatrix} = \begin{vmatrix} \hat{n}_1(\lambda+2\mu)\partial_1 u_1 + \hat{n}_2\mu\partial_2 u_1 + \hat{n}_1\lambda\partial_2 u_2 + \hat{n}_2\mu\partial_1 u_2 \\ \hat{n}_1\mu\partial_2 u_1 + \hat{n}_2\lambda\partial_1 u_1 + \hat{n}_2(\lambda+2\mu)\partial_2 u_2 + \hat{n}_1\mu\partial_1 u_2 \end{vmatrix} \tag{15}$$

We chose to solve eq. (4) in the spatial dimension using multiquadratic radial basis functions, which are defined as

$$\phi(\boldsymbol{x}) = \sqrt{1 + (\epsilon|\boldsymbol{x} - \boldsymbol{x}_o|)^2}. \tag{16}$$

In the above equation ϵ is the shape parameter and $\boldsymbol{x}_o$ is the center of the RBF. We chose to use multiquadratic radial basis functions because interpolating a function using $\phi(\boldsymbol{x})$ has the desirable trait of being equivalent to piece-wise linear interpolation for $\epsilon \to \infty$ and polynomial interpolation for $\epsilon \to 0$ at least for one-dimensional problems (Driscoll & Fornberg, 2002). This suggests that a wide range of values for ϵ should produce reasonably accurate results because either end-member is a perfectly valid means of interpolation. This is in contrast to using RBFs that decay to zero as $|\boldsymbol{x} - \boldsymbol{x_o}| \to \infty$, where the interpolant for $\epsilon \to \infty$ is essentially useless. We follow the common practice of making ϵ for each RBF proportional to the distance to the nearest RBF center. We did not rigorously search for an optimal proportionality constant; however, we note that we tend to get unstable or obviously inaccurate solutions for proprtionality constants greater than 2 and less than 0.1. For the solution presented in this paper, we used a proportionality constant of 1, that is, we set ϵ equal to the distance to the nearest neighbor.

We approximate the solution for displacements as

$$u_1 \approx \sum_{j=1}^{N} \alpha_j(t)\phi_j(\boldsymbol{x}) \tag{17}$$

and

$$u_2 \approx \sum_{j=1}^{N} \beta_j(t)\phi_j(\boldsymbol{x}), \tag{18}$$

which can also be written as

$$\begin{vmatrix} u_1 \\ u_2 \end{vmatrix} \approx \boldsymbol{G} \begin{vmatrix} \boldsymbol{\alpha} \\ \boldsymbol{\beta} \end{vmatrix} \tag{19}$$

where $\boldsymbol{G}$ is given by

$$\boldsymbol{G} = \begin{vmatrix} \boldsymbol{\phi} & \mathbf{0} \\ \mathbf{0} & \boldsymbol{\phi} \end{vmatrix} \tag{20}$$

and we are no longer explicitly writing the time and space dependence. We can then express acceleration in terms of the spectral coefficients, $\boldsymbol{\alpha}$ and $\boldsymbol{\beta}$, as

$$\begin{vmatrix} \partial^2 u_1/\partial t^2 \\ \partial^2 u_2/\partial t^2 \end{vmatrix} = \boldsymbol{H} \begin{vmatrix} \boldsymbol{\alpha} \\ \boldsymbol{\beta} \end{vmatrix} + \begin{vmatrix} f_1 \\ f_2 \end{vmatrix}, \tag{21}$$

where

$$\boldsymbol{H} = \begin{vmatrix} \partial_1\left((\lambda+2\mu)\partial_1\boldsymbol{\phi}\right) + \partial_2\left(\mu\partial_2\boldsymbol{\phi}\right) & \partial_1\left(\lambda\partial_2\boldsymbol{\phi}\right) + \partial_2\left(\mu\partial_1\boldsymbol{\phi}\right) \\ \partial_1\left(\mu\partial_2\boldsymbol{\phi}\right) + \partial_2\left(\lambda\partial_1\boldsymbol{\phi}\right) & \partial_2\left((\lambda+2\mu)\partial_2\boldsymbol{\phi}\right) + \partial_1\left(\mu\partial_1\boldsymbol{\phi}\right) \end{vmatrix}. \tag{22}$$

The boundary conditions can also be expressed in terms of the spectral coefficients as

$$\begin{vmatrix} 0 \\ 0 \end{vmatrix} = \boldsymbol{B} \begin{vmatrix} \boldsymbol{\alpha} \\ \boldsymbol{\beta} \end{vmatrix}, \tag{23}$$

where

$$\boldsymbol{B} = \begin{vmatrix} \hat{n}_1(\lambda+2\mu)\partial_1\boldsymbol{\phi} + \hat{n}_2\mu\partial_2\boldsymbol{\phi} & \hat{n}_1\lambda\partial_2\boldsymbol{\phi} + \hat{n}_2\mu\partial_1\boldsymbol{\phi} \\ \hat{n}_1\mu\partial_2\boldsymbol{\phi} + \hat{n}_2\lambda\partial_1\boldsymbol{\phi} & \hat{n}_2(\lambda+2\mu)\partial_2\boldsymbol{\phi} + \hat{n}_1\mu\partial_1\boldsymbol{\phi} \end{vmatrix}. \tag{24}$$

At this point, all the information in $\boldsymbol{G}$, $\boldsymbol{H}$, $\boldsymbol{B}$, and $\boldsymbol{f}$ are given by the problem description or are user defined variables. Finding the spectral coefficients for $\boldsymbol{u}$ is then straightforward. We perform the time integration with a leapfrog method and our procedure for solving eq. (4) is as follows:

1. Form the matrix $\boldsymbol{J}$, which consists of $\boldsymbol{B}$ evaluated at the boundary collocation points and $\boldsymbol{G}$ evaluated at the interior collocation points.
2. Form the vector $\boldsymbol{r}^0$, which consists of zeros for the boundary collocation points and $\boldsymbol{u}^0$ at the interior collocation points
3. Solve $\boldsymbol{r}^0 = \boldsymbol{J}[\boldsymbol{\alpha}^0\ \boldsymbol{\beta}^0]^T$ for $\boldsymbol{\alpha}^0$ and $\boldsymbol{\beta}^0$
4. evaluate the initial acceleration, $\boldsymbol{a}^0$, using eq. (21)
5. begin time stepping
   (a) evaluate $\boldsymbol{u}^t = \boldsymbol{u}^{t-1} + \boldsymbol{v}^{t-1}\Delta t + \boldsymbol{a}^{t-1}\Delta t^2$
   (b) Form $\boldsymbol{r}^t$
   (c) Solve $\boldsymbol{r}^t = \boldsymbol{J}[\boldsymbol{\alpha}^t\ \boldsymbol{\beta}^t]^T$ for $\boldsymbol{\alpha}^t$ and $\boldsymbol{\beta}^t$
   (d) evaluate $\boldsymbol{a}^t$ from eq. (21)
   (e) evaluate $\boldsymbol{v}^t = \boldsymbol{v}^{t-1} + 1/2(\boldsymbol{a}^{t-1} + \boldsymbol{a}^t)\Delta t$

There are, however, a few additional details that need to be addressed. First, we must deal with the material properties, μ, λ, and ρ. We use the material properties from the Preliminary Reference Earth Model (PREM) (Dziewonski & Anderson, 1981). PREM was inferred using observed P and S wave travel times in addition to other geophysical data. We then have a means of validating our numerical solution because the travel times predicted by our numerical simulation should be consistent with observable travel times. The material properties for PREM are given at discrete depths, and so we perform an interpolation

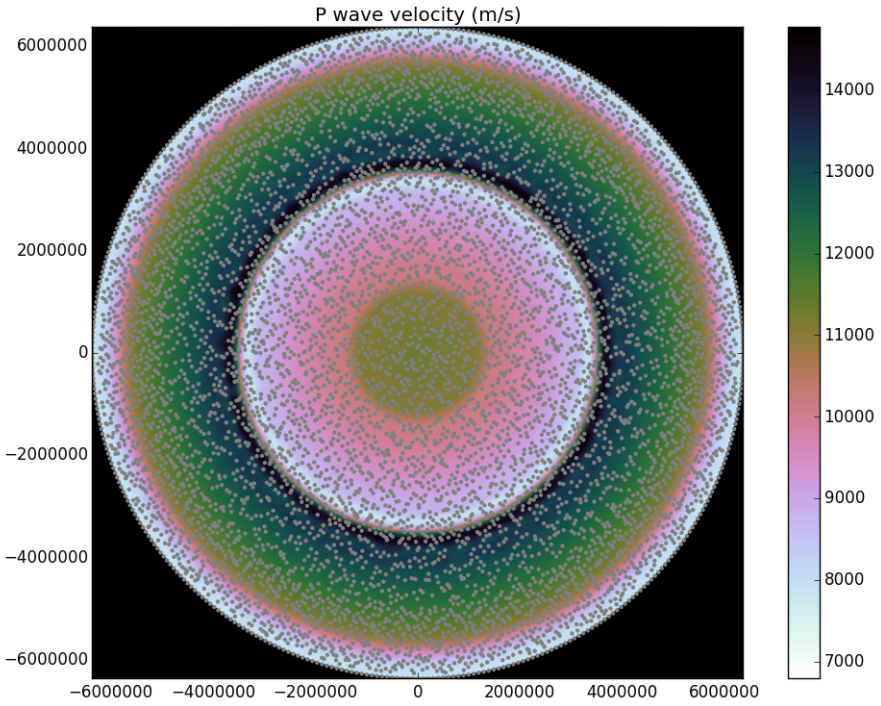

Figure 2: P wave velocities ($\sqrt{(\lambda + 2\mu)/\rho}$) from PREM. Gray dots indicate collocation points used in solving eq. (4)

using multiquadratic RBFs to obtain PREM as a continuous and analytically differentiable function. Our interpolants for PREM are shown in figure 2, 3, and 4.

We also must address how the collocation points are chosen. PREM has a major material disontinuity at the core-mantle boundary and we would ideally prefer to have a higher density of nodes at that interface. Additionally, the lower mantle has higher P and S wave velocities relative to the upper mantle, crust, and core. We would then prefer a lower density of collocation points in the lower mantle in order to keep our solution stable during time stepping. Although we seek regional scale variations in node density, we still want our collocation points to have low discrepency in any given region of the earth. We have developed a simple method to produce a distribution of collocation points that satisfy our specifications. Let $\psi : \boldsymbol{x} \to [0, 1]$ be a normalized function describing the desired density of collocation points at position $\boldsymbol{x}$. Let H_k^1 be the k^{th} element in a one-dimensional Halton sequence. Let H_k^2 be the k^{th} element of a two-dimensional Halton sequence which has been scaled so that H_k^2 can lie anywhere in the problem domain, D. The set of N collocation points, $\boldsymbol{C}$, with the desired density can then be found with algorithm 1.

In our experience, we found that it is necessary to have a small buffer between the boundary collocation points and interior collocation points. This is essential for a stable solution. We take the width of the buffer to be the smallest distance between boundary nodes. The reader may be able to notice this slight buffer in either Figures 2, 3 or 4.

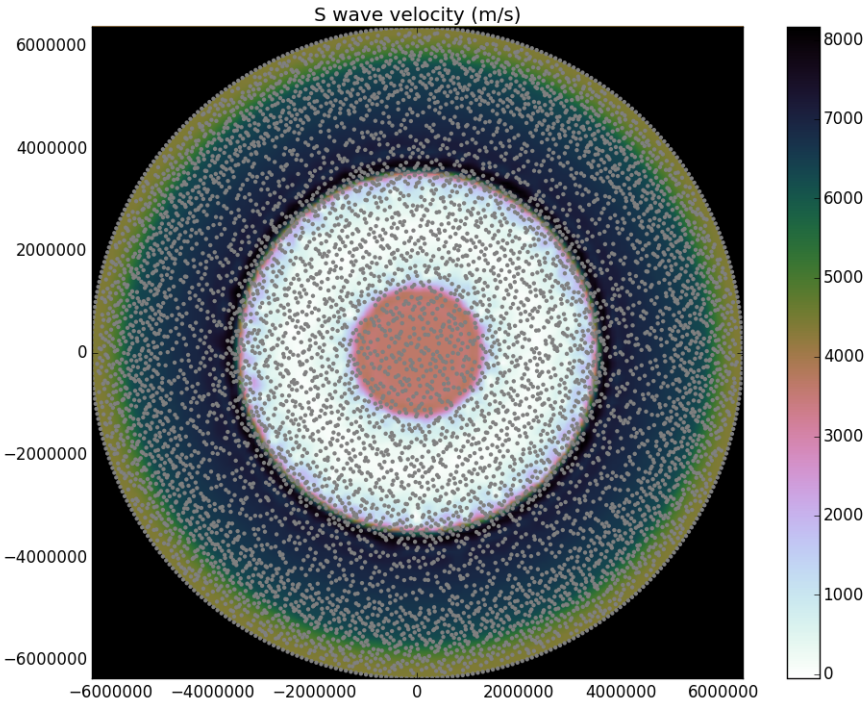

Figure 3: S wave velocities ($\sqrt{\mu/\rho}$) from PREM

Algorithm 1 Collocation points

$\boldsymbol{C} = \emptyset$
$k = 0$
while (length of $\boldsymbol{C}$) $< N$ **do**
  if $(\phi(H_k^2) > H_k^1) \& (H_k^2 \in D)$ **then**
    append H_k^2 to $\boldsymbol{C}$
  end if
  $k = k + 1$
end while

Results

Our numerical solution to eq. (4) is shown in figures 2-10. The most prominent feature in our solution are the Raleigh waves which travel along the surface and have decaying amplitude with depth. The fastest traveling waves are the P waves which have only a faint signature. We can also be assured that the material properties are properly implemented because S waves, which have displacements parallel to the wave front, do not enter the core because it has a shear wave velocity of zero.

It is also worth noting that the solution has symmetry about the vertical axis. This symmetry is no suprise and we have attemted to solve eq. (4) on only half the domain.

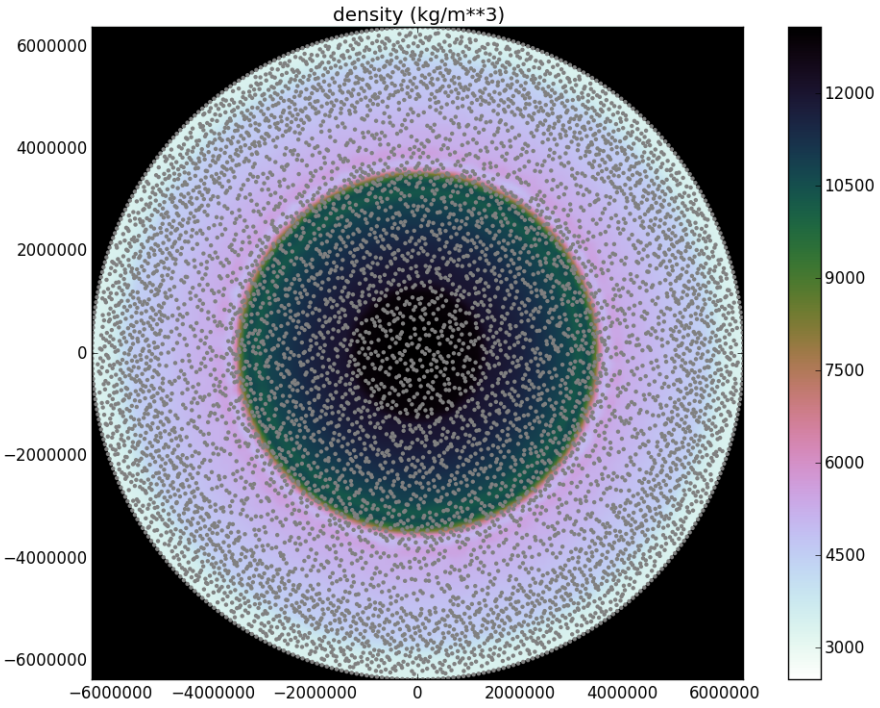

Figure 4: Densities from PREM

However, we have found that solutions using RBFs are incredibly sensitive to corners in the domain and our solution quickly went unstable after a few time steps.

We note that the magnitude of displacements in our solution is far larger than what we would reasonably expect. We believe this to be a bug in our program that is related to unit conversions and the actual solution should be different by only a constant factor.

We can also verify the accuracy of our solution by ensuring that it is symmetric

When

We set the distance between the force couples, d, to 500 km. The value of d is

We use 8000 collocation points and solve for displacements

Complications

Representing an infinitesimally small source is difficult

Corners suck

cfl criteria holds strong

consider iterative solvers

Seems to be stable for Poisson solids

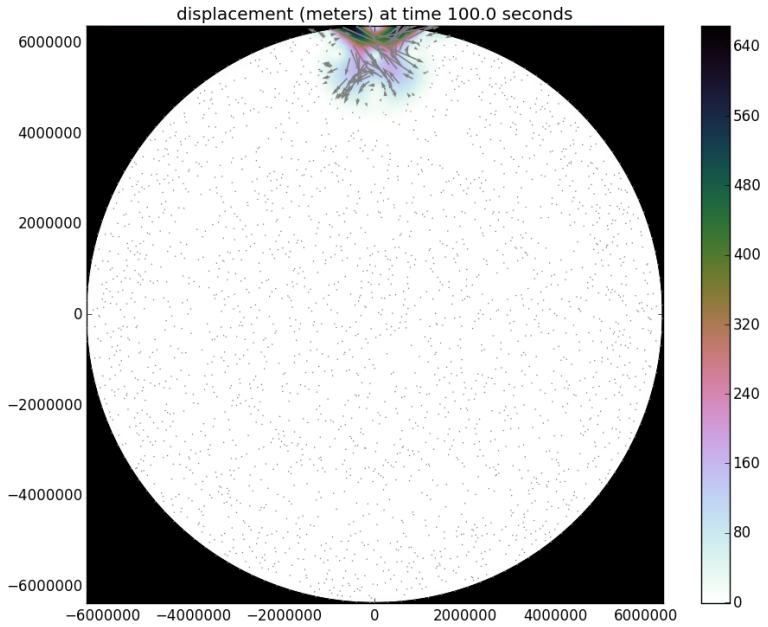

Figure 5: Solution for displacements at 100 seconds after an earthquake. Color indicates the magnitude of displacement and vectors indicate direction

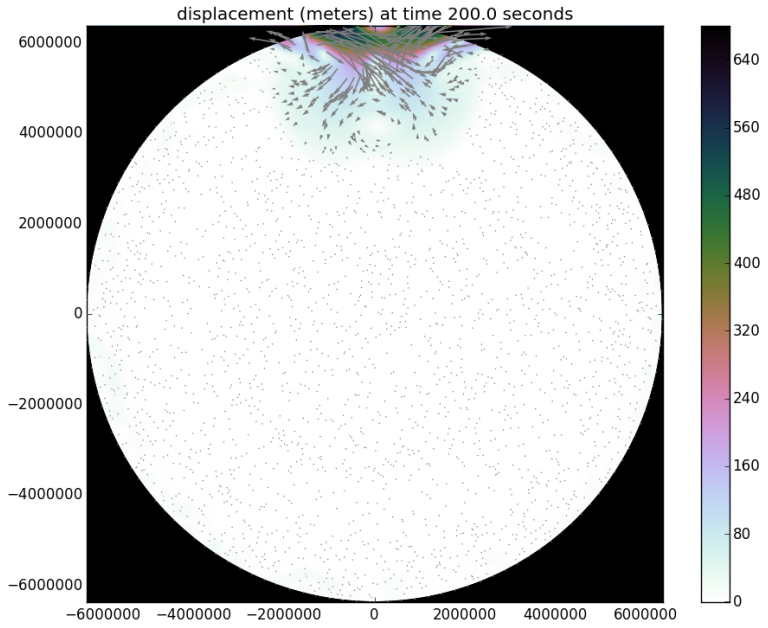

Figure 6: Solution for displacements at 200 seconds after an earthquake

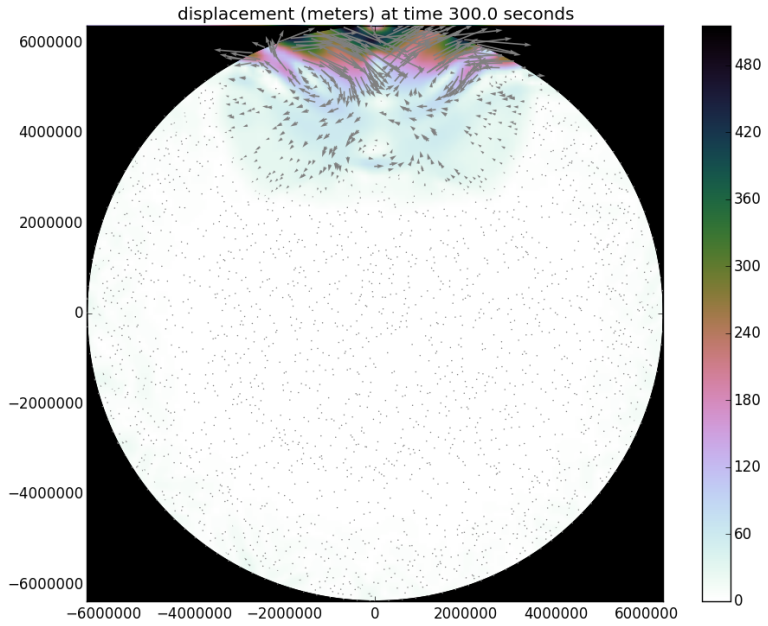

Figure 7: Solution for displacements at 300 seconds after an earthquake

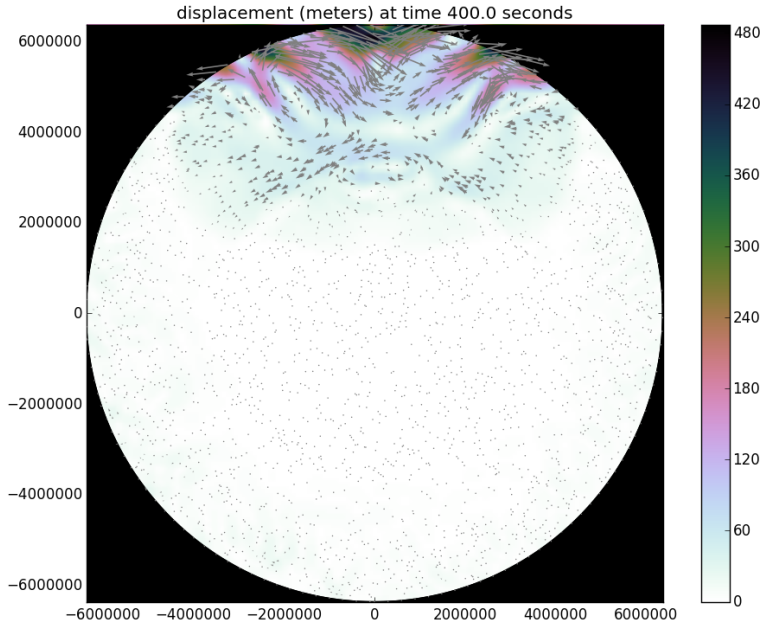

Figure 8: Solution for displacements at 400 seconds after an earthquake

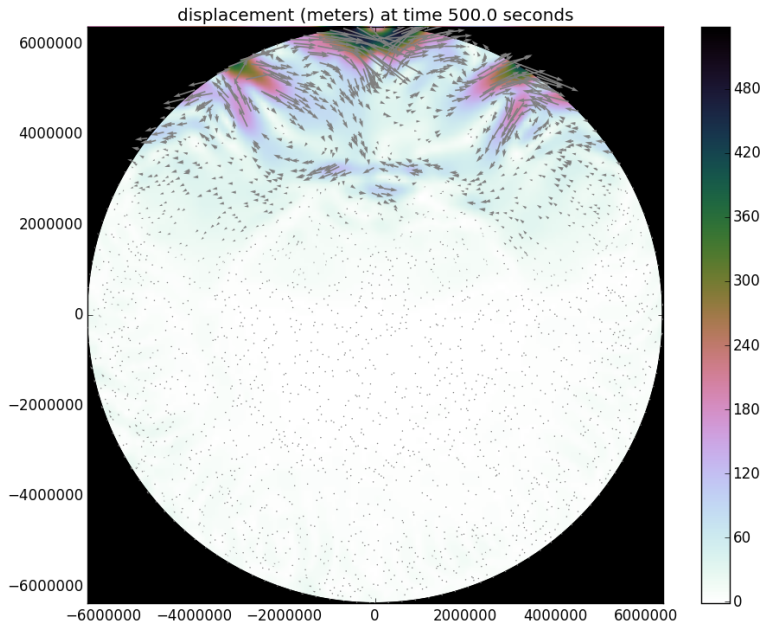

Figure 9: Solution for displacements at 500 seconds after an earthquake

Additional Notes

Domain Geometry
: Seems to be stable only for Poisson solids

Additional notes

All the software that I have written to produce the results shown in this paper are included below. The software (with eventual bug fixes) can also be found at https://github.com/treverhines/SeisRBF My software uses packages which can be found in the Anaconda Python distribution from Continuum Analytics.

References

Aki, K. & Richards, P., 2002. Quantitative Seismology, second edition, *University Science Books*

Driscoll, T. & Fornberg, B., 2002. Interpolation in the limit of increasingly fiat radial basis functions, *Computers and Mathematics with Applications*, 43, 413-422.

Dziewonski, A. M. & Anderson, D.L., 1981. Preliminary reference Earth model. *Phys Earth Planet Inter*, 25, 297-356. doi:10.1016/0031-9201(81)90046-7.

Fichtner, A., 2011. Full Seismic Waveform Modelling and Inversion, *Springer*